Kidney International, Vol. 55 (1999), pp. 400–416

PERSPECTIVES IN BASIC SCIENCE

The development of x-ray imaging to study renal function

Lilach O. Lerman, Martin Rodriguez-Porcel, and J. Carlos Romero

Department of Physiology and Biophysics, Mayo Clinic and Foundation, Rochester, Minnesota, USA

The development of x-ray imaging to study renal function. The well-established role of the kidney in control of blood volume and ultimately arterial blood pressure has been underscored by the demonstration of alterations in renal hemodynamics and function recognized as responsible for these and other regulatory mechanisms. Nevertheless, the spatial complexity of intrarenal structure and function has made evident the need to study these separately in different regions of the intact kidney. Because of the introduction of x-rays, assessment of renal function has indeed been one of their attractive applications. However, despite the appeal of their noninvasiveness, several limitations confounded the different x-ray techniques used, most of which remained unresolved until the development of computed tomography. Furthermore, the development of fast imaging, which allows repetitive analysis of the same region of interest during the transit of contrast medium, holds a great potential to estimate intrarenal distribution of blood flow and the dynamic characteristics of tubular fluid flow in individual nephron segments. This latter assessment requires the administration of filterable x-ray contrast medium, which is cleared from the plasma almost exclusively by glomerular filtration, and the generation of contrast dilution curves. A historical review of the development and progress of the various x-ray techniques used will help understand the past and present of x-ray imaging, and will make it easier to envision the importance of their future roles in the study of renal physiology and pathophysiology.

Approximately 100 years ago, in 1895, Wilhelm Conrad Roentgen discovered x-rays, a technique that revolutionized clinical medicine throughout this century because it allowed, for the first time, a nonsurgical visualization of the internal anatomy of the human body [1]. In the early years, most efforts were directed toward defining the characteristics of x-ray images reflecting specific pathological processes such as intestinal obstruction, cerebral hemorrhage, dissecting aneurysm, etc. However, in the 1920s, the success of a technique called "excretory urography," using sequential x-ray images in conjunction with contrast media to explore renal excretory function, strongly suggested that x-rays could be used to obtain dynamic information about renal function [2]. The assessment of organ function implies evaluation of a specific dynamic characteristic, which in the kidney may be attributed to renal circulation, glomerular filtration rate, or tubular dynamics. The advances made in x-ray image reconstruction have enhanced resolution and facilitated estimation of these parameters in great detail [3]. For example, assessment of the renal circulation is no longer limited to the measurement of global renal blood flow but has been expanded to the estimation of intrarenal regional distribution of blood to specific areas of the superficial, middle, or deep cortex or in the outer or inner medulla. Likewise, the glomerular filtration rate can be indirectly estimated in different areas of the renal cortex, and the transit of fluid through different nephron segments, as well as fluid reabsorption, can be assessed in the *in vivo* intact kidney. These capabilities of x-ray and contrast media will considerably enhance the ability of the clinician to achieve a more accurate diagnosis of renal diseases and to pinpoint early and subtle defects in the evolution of renal pathology, such as those preceding overt hypertension. Therefore, the objective of this review is to trace the historical development of x-rays with special emphasis on their utilization to evaluate functional parameters. We believe that these new applications will revolutionize the diagnostic and follow-up procedures in nephrology.

Key words: x-rays, computed tomography, contrast media, contrast dilution curves, non-surgical visualization, diagnosis of renal disease.

Received for publication July 24, 1997
and in revised form April 6, 1998
Accepted for publication April 6, 1998

PRINCIPLES OF X-RAY IMAGING

Since the discovery of x-rays by Roentgen in 1895 [1, 4], there has been a progressive technological sophistication that has made possible not only a better exploration of different organs, but the transversal section of the body and, finally, the study of functional characteristics.

The most common modes of x-ray imaging techniques that have been used for renal studies can be divided into three major categories: projection radiography, linear (axial) tomography, and computed (transaxial) tomography (CT; Fig. 1). Technical aspects of historical or conventional methods are only briefly summarized in this

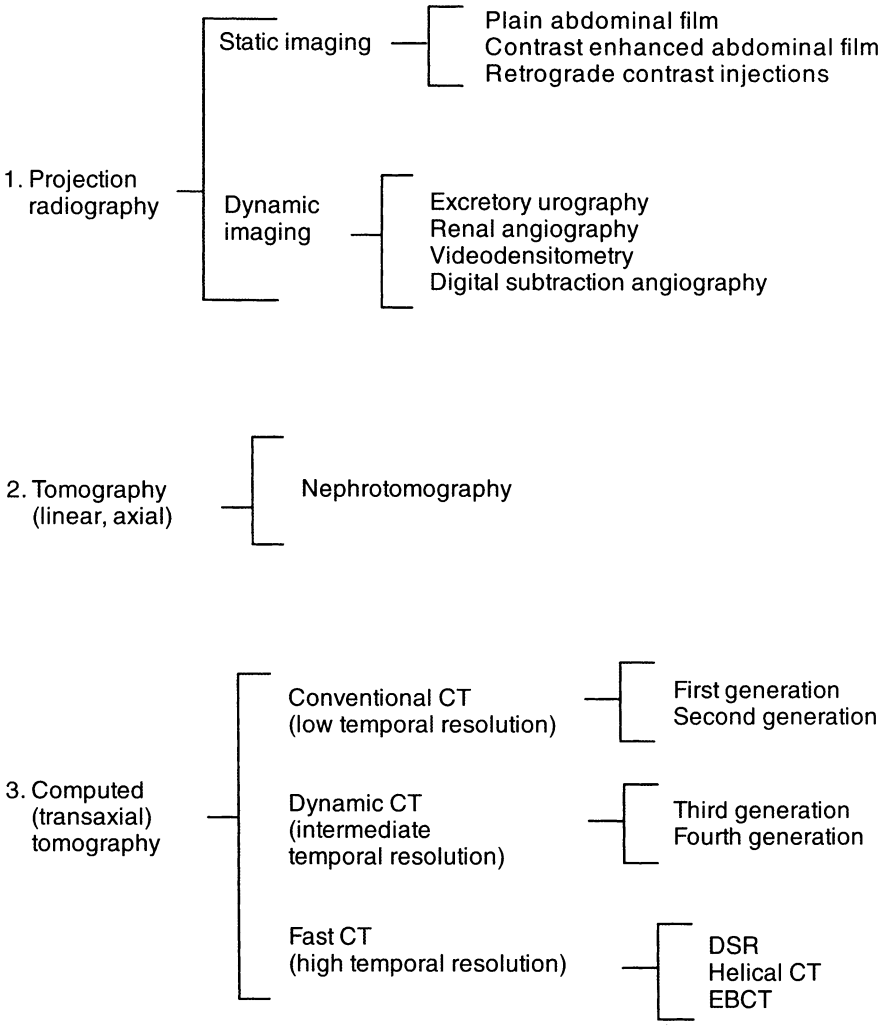

Fig. 1. Flow chart describing major categories of x-ray imaging techniques used to study renal physiology and pathophysiology. Abbreviations are: CT, computed tomography; DSR, dynamic spatial reconstructor; EBCT, electron beam CT.

review, whereas a greater emphasis is placed on more sophisticated and novel techniques developed with CT.

PROJECTION RENAL RADIOGRAPHY

Projection renal radiography derived its name from the mode of image acquisition, with the x-ray source and the film being stationary (Fig. 2, left panel), and all of the points in the path of any x-ray projected on the same point on the film. The images generated by this technique have been used for virtually a century to outline the major characteristics of gross renal anatomy and pathology, and are still useful today. The two major categories of projection radiography are conventionally classified as static and dynamic imaging.

Static imaging

For the first 30 years after their inception, renal radiography was mostly circumscribed to assessment of anatomical structures [5]. In 1896, the first plain abdominal film, describing renal and ureteral calculi, was obtained [6]. This first attempt was followed by various enhancement techniques, such as placement of a metal stylet in the ureter [7] or the use of barium and other radiopaque substances [8] which were used to facilitate visualization of the urinary system [9]. Similarly, ureteral retrograde injections of contrast media were used to diagnose neoplasms, chronic pyelonephritis, congenital abnormalities, and cystic processes. This procedure constituted an important step in the radiological evolutionary process but had several limitations, the main of which was a high incidence of renal infection (for example, pyelonephritis).

Dynamic imaging

Excretory urography. The first important attempt to explore the excretory function of the kidney was undertaken in 1923 by Earl Osborne, who developed intravenous pyelography at the Mayo Clinic [10]. This investigator based his technique on the observation that iodine

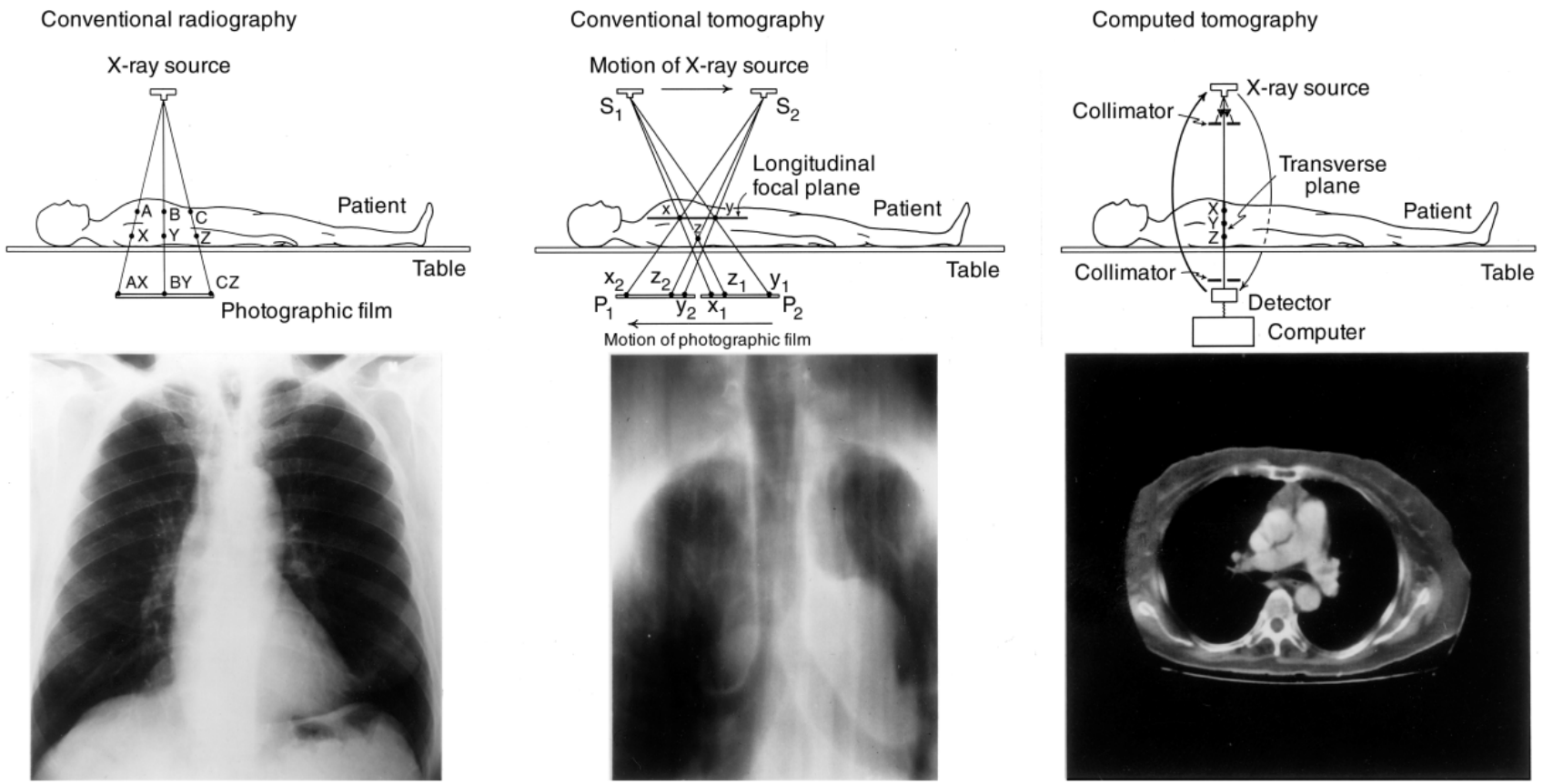

Fig. 2. Schematic representation of acquisition technique of projection radiography (left), linear tomography (center), and CT (right). (From Robb RA: X-ray CT: An engineering synthesis of multiscientific principles. *CRC Crit Rev Biomed Eng* 7:265–334, 1982; used with permission.)

compounds were easily detectable by x-rays during their renal clearance. This method allowed, for the first time, the study of renal function [11]. Other attempts included retroperitoneal air instillation [2] and nephrotomography [12]. The former was based on the concept that air in the retroperitoneal space will enhance the kidney and adrenal shape shadows [2], whereas the latter combined the use of intravenous pyelography with body section roentgenography [12], in an attempt to exclude surrounding abdominal contents from the region of interest.

Angiography. Renal circulation has also been a main focus of interest when studying renal function. Angiography is a technique used to examine changes in the luminal diameter of the vascular tree by application of x-rays during vascular transit of contrast media, making it very useful in the diagnosis of renal artery stenosis. Trueta et al, who were the first to perform a dynamic renal angiography study, carefully timed their x-ray picture shooting and were able to recognize the transit of contrast through the renal artery and intrarenal branches in the cortex, as well as through the medulla and the renal vein [13]. The contrast medium (Thorotrast®) was a colloidal substance, nonfiltered by the glomeruli, which provided good intravascular radiopacity characteristics.

These experiments constituted a milestone in the study of renal function, as it was the first time renal circulation was dynamically studied with the aid of x-rays. Furthermore, in another set of studies, this group of investigators was the first to describe the phenomenon of independent regulation of cortical and medullary blood flow, which they interpreted as possible blood shunting between different regions of the kidney [13]. The physiological and pathophysiological significance of these findings is discussed later in this article.

Videodensitometry. The reliability of measurement of renal function with substances that are eliminated by the kidney depends to a great extent on the accuracy with which the amount of the excreted substance can be quantitated. This issue was addressed with the introduction of videodensitometry. Densitometry is a technique capable of obtaining measurements of the concentration (density) of roentgenographic contrast media in the circulatory system through analysis of time/density curves by measuring "brightness" at selected areas of the x-ray images. The name videodensitometry reflects improvement in this technique achieved by the addition of video analysis and storage capabilities [14, 15].

Erikson et al were the first to apply this methodology to study renal parenchymal perfusion [16] and function [17]. They performed a videodensitometric study of the kidney after injection of a glomerular filterable contrast medium (Angiografin®) and repeated it after injection of a nonfilterable, intravascular contrast medium (Thorotrast®). Erikson et al found that the two types of contrast media resulted in different time-density curves: The concentration curve of the intravascular marker Thorotrast® returned to basal levels after its passage through the vascular compartment of the kidney (Fig. 3A), whereas the curve obtained with the filterable Angiografin® had a tail of "residual opacity" lingering above baseline levels (Fig. 3B) [16]. They attributed that difference to the fact that Angiografin® was being filtered by the glomeruli and retained in the tubules, whereas Thorotrast® was completely washed out via the renal vein. Subtraction of the Thorotrast® curve from the Angiografin® curve yielded a new curve representing the amount of filtered contrast retained in the tubular compartment after the vascular passage (filtration curve; Fig. 3B). From this curve, they estimated filtration fraction as a function of residual opacity divided by the maximal height of the vascular curve [16].

The two important advantages of this technique were (*a*) the assessment of renal blood flow and tubular dynamic with the use of two injections of contrast, and (*b*) the possibility of calculating blood flow, without requiring sampling of the actual tissue contrast concentration. In spite of some limitations, videodensitometry was the first method to evaluate renal function using x-ray imaging, a concept that is further developed in subsequent sections when discussing novel imaging techniques.

Digital subtraction angiography. This method, introduced in the 1980s, combines routine angiography (visualization of vascular lumen) with computer software capable of digitizing and analyzing the signal received from the kidney during the passage of contrast media injected intra-arterially or intravenously [17, 18]. After appropriate background subtraction and processing, it allows characterization of the signal produced by the contrast medium alone during its renal passage. This method is very useful to assess severity of renal arterial stenosis, as part of the work-up of hypertensive patients, but does not provide information on renal parenchymal perfusion. The major problem with this method is related to the accuracy with which one can focus on the renal artery. The need for this was obviated with the introduction of body section roentgenography, in which the tomographic image is constructed by combining data obtained from a multitude of different views [17]. This approach is discussed in the following sections.

LINEAR (AXIAL) TOMOGRAPHY

The name *tomography* derives from the Greek words *tome* (to cut) and *graphein* (to write). The principle on which tomography is based was borrowed from optics, in which the x-ray tube and the film are moved synchronously in opposite directions during exposure, whereas the object is kept motionless (Fig. 2, center panel) [19]. Some important modifications have been introduced over the years. For example, in 1930, Valebona intro-

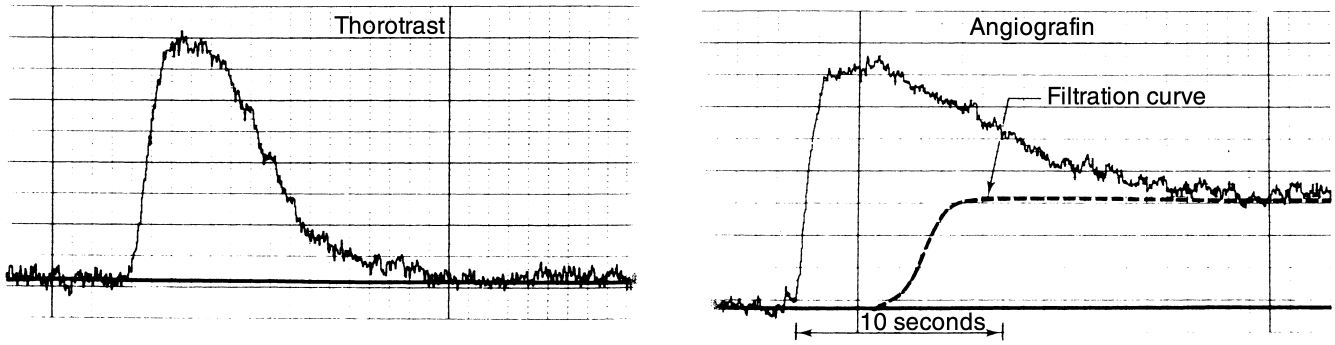

Fig. 3. (*A*) Videodensitometric curve obtained after the injection of an intravascular contrast agent (Thorotrast®). Note the return of renal density to baseline level following contrast washout. (*B*) Videodensitometric curve obtained after injection of a filterable contrast agent (Angiografin®), whose tubular retention led to a "tail" of residual opacity. The dotted line shows the filtration curve obtained by subtracting the Thorotrast® curve from the Angiografin® curve. (From Erickson U, Lorelius LE, Rhun G, Wolfgast M: Regional renal function measured by videodensitometry. *Scand J Nephrol* 15:131–135, 1981; used with permission.)

duced *autotomography*, in which the x-ray source and the film are stationary, with the object being the moving part [20]. Using this technique, objects located in the plane under study are clearly visualized, whereas moving parts appear blurred in the image. The initial application of this technique was limited to the bronchopulmonary system [21].

The use of axial tomography in nephrology was mainly through a technique called nephrotomography [12], in which consecutive pictures of the kidneys were taken following a nephrogram phase (phase of renal excretion of a preinjected substance). The major limitation was that only a single plane could be identified at a time, and only a limited region was clear in the film, the rest appearing blurred [20]. This made impossible a complete analysis of the cross-section being studied. In multisection tomography, several sections of the body could be obtained with one radiation exposure (by placing different films at different distances from the source). However, none of them were as reliable as a "single cut" study, the latter often being required as a supplementary view [22, 23]. These problems were largely addressed with the advent of CT (transaxial).

COMPUTED TOMOGRAPHY (TRANSAXIAL)

Image reconstruction

Computed (transaxial) tomography (CT; Fig. 2, right panel) is based on the mathematical concept known as image reconstruction, developed in 1917 by J. Radon, who derived a formulation to reconstruct an object from its different projections in space [23]. This investigator proved that two- and three-dimensional objects can be reconstructed from an infinite set of projections. In the late 1950s and 1960s, Oldendorf [24], Cormack [25], and Hounsfield [26] adapted such mathematical techniques to make transaxial reconstructions, which culminated in the development of CT in 1973 [26].

To demonstrate this basic principle, Figure 4 shows the basic operations underlying reconstruction of a transverse section of a cross-shaped object using two (orthogonal) x-ray projections oriented perpendicular (90° rotation) to the arms of the cross. Variations in the opacity of the projections, which are determined by the thickness of the cross segment interposed in the x-ray pathway, can be recorded as such in an x-ray film, represented in Figure 4 by an open square. The opacity of the projection can also be recorded as an analog signal by photo cells aligned along the same transverse plane. This is shown in Figure 4, in which the analog displays curves reaching the values 3 and 1, corresponding to the same x-ray density of the back projections recorded in the film. The summation of the opacities recorded from the two projections illustrated in Figure 4 can also be represented (digitized) by a numerical set of values from which the transversal section of the cross can be reconstructed. In this simplified example, a partially blurred two-dimensional reconstruction of the cross is obtained, and the corresponding digitalization is heterogenous. This low accuracy of reconstruction resulted mainly from the limited angles of projection (views) used to scan (describe) and reproduce the original object. It is important to mention here that the summation method used in our example is a very simplified version of the so-called filtered back-projection technique. There are, however, other methods for reconstructing images that involve algebraic reconstruction and the Fourier analysis-based method, a description of which is beyond the scope of this review.

Once the tomographic images are reconstructed, most organs can be identified in the cross-sectional images by their unique shapes and locations, as well as by differential tissue densities. To study the kidney, although it

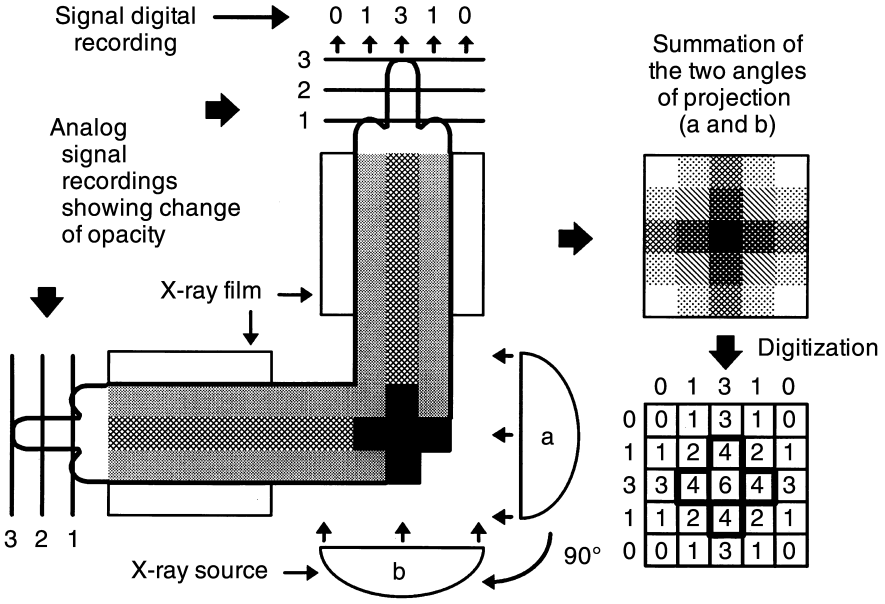

Fig. 4. Procedure for generation of multidimensional attenuation profiles (see text).

is sometimes distinguishable from surrounding tissues without the need for contrast media, their administration is necessary in order to distinguish between the cortex and medulla, which have similar baseline tissue densities (CT numbers). Because the cortex receives the majority of renal blood flow [27], administration of contrast media is followed by marked cortical enhancement (that is, increase in CT numbers) so that the corticomedullary border is easily discernible. Indeed, for several years, the radiological application of CT was limited to anatomic studies. In 1980, Axel was the first to suggest the use of CT-derived changes in tissue density to calculate cerebral blood flow [28]. Similar principles have since been adapted for calculation of renal blood flow. One of the greatest advantages of x-ray contrast media over those used in conjunction with other imaging modalities (such as ultrasound, magnetic resonance imaging, and radionuclear methods), the concentration of x-ray contrast media in a tissue is linearly related to tissue radio density in the dynamic range usually used in clinical imaging [3, 29]. Consequently, determination of changes in tissue density reflects proportional changes in concentration of contrast in the region of interest, and measurements of blood or filtrate flow are quantitative rather than qualitative. Although positron emission tomography scanning also provides accurate measurements of renal perfusion [30], the superior spatial resolution of CT enables this to be measured in different, small regions of the kidney. Recording the transit of contrast by repeated scanning throughout its transit in the renal vascular compartment enables estimation of renal perfusion. Following the glomerular filtration and tubular transit of contrast provides a measure of renal function.

Therefore, analysis of CT images in conjunction with contrast pharmacokinetics can be used to calculate renal size, blood flow, and function.

Calculation of renal volume

To measure renal volume using tomographic images, the kidney is usually scanned from pole to pole by moving the subject table at equal consecutive increments, and cross-sectional images are obtained. Renal contours can be subsequently identified and manually traced on each image. Following the identification of the corticomedullary junction on each image, the cortex and medulla can also be independently traced and the area enclosed within the trace calculated. Multiplication of the calculated area of a region by tomographic slice thickness yields the volume of the region of interest on that image; summation of regional volumes calculated from all the images would yield the total volume of that region (Simpson's rule). A statistical random-marking method has also been validated for volume calculation from CT images [31, 32], and the volume estimations it provides are very close to those obtained using manual tracing.

Because of the curvature of the renal surface, a tomographic slice with a finite thickness may include constituents of different densities in the same voxel (picture volume element), with the resultant voxel density being an average of those constituents sampled [33]. This artifact, termed partial volume or volume averaging effect, can be substantially reduced by using thin (6 mm or less) tomographic slices. The desirable decrease in slice thickness is, however, limited by a decrease in the signal-to-noise ratio when fewer photons are detected per voxel [3].

The ability to distinguish visually between different

renal structures and the degree of imaging artifacts varies with the spatial and density resolution of the CT scanner.

The spatial resolution of a scanner, which is the ability to visually distinguish small, high-contrast objects in an image, is typically measured with a phantom with line-pair patterns of variable spatial frequency. Low-contrast resolution, on the other hand, is the ability to distinguish objects in which the density differs little from their surrounding background material and is determined using objects embedded in a phantom of a similar density. The image noise, created by random fluctuation of CT numbers in an image of a uniform object, is directly related to radiation exposure, that is, the number of photons used to create the image [34]. All of these image-quality parameters can therefore affect the accuracy with which the kidney is discerned from surrounding structures or the corticomedullary border defined.

Calculation of renal perfusion and flow

Flow studies using CT are usually based on sequential scanning of the same tomographic level during the transit (first pass) of a bolus of contrast media. Since tissue density is linearly related to contrast concentration [35] and the contrast is assumed to be well mixed with blood (which is especially true after intravenous injections) [33], flow of contrast to a perfused tissue will follow the distribution of blood and will result in a parallel increase in the density (CT numbers) of the tissue. The change in tissue density (representing a change in contrast concentration) can be plotted against time, and through the application of mathematical algorithms, regional perfusion (in units of ml blood/min/cc tissue) can be assessed according to the principles of the indicator-dilution theory [33], using parameters such as the area under the time-density curve, its peak height, and the mean transit time of contrast through the region of interest. To obtain blood flow (in units of ml blood per min), perfusion values are multiplied by regional volume calculated separately, as discussed earlier.

To ensure faithful description of the time-density curve, scan duration needs to be short, preferably under a second, so that minimal changes will occur during scan acquisition time. Moreover, interscan delays should be short, preferably no longer than one to two seconds, to enable a high repetition rate and adequate sampling of the rapid density changes taking place during the transit of contrast in the vascular compartment. The accuracy of these measurements is therefore greatly dependent on the temporal resolution of the CT scanner used.

Short scan durations also offer the advantage of freezing anatomical motion and minimizing motion artifacts. The trade-off of high temporal resolution, however, is a decrease in the number of photons measured by the detectors and thereby increased noise levels. The choice between high spatial and temporal resolution depends on the capability of the scanner and on the specific clinical application [34].

Calculation of renal function

Urographic contrast media are extracellular markers that are removed from circulation primarily via glomerular filtration and are not secreted or reabsorbed in the kidney [36]. In that regard, they behave like inulin [37], with the advantage that their intrarenal concentration can be externally detected and quantitated using CT scanning [38], and their kinetics subsequent to vascular transit provide a measure of renal function.

Different approaches have been attempted to determine indices of renal function using CT. Renal clearance of contrast has been estimated by documenting the decrease in soft tissue density over a period of a few hours, which was inconveniently time consuming [37, 39]. Therefore, sequential renal scanning during a single, first pass of a bolus of contrast through the kidney has been attempted and applied in several ways. In 1981, Ishikawa et al were the first to study CT-derived renal time-density curves [40]. In the 1980s, the intersection time of cortical and medullary curves (corticomedullary junction time) during a first pass of a bolus of contrast through the kidney has been subsequently used as a semiquantitative measure of renal concentration ability [41, 42]. More recently, the residual opacity of contrast was used to assess filtration fraction [43, 44], and changes in density of the whole kidney during a first-pass of contrast was used in an attempt to calculate renal permeability and glomerular filtration rate, by adaptation of mathematical analysis designed to calculate renal permeability [45] and glomerular filtration rate [39, 46], by adaptation of mathematical analysis designed to calculate the permeability of the blood–brain barrier [47]. Although promising, this methodology requires further validation against independent measures of renal function. Finally, recording the flow of contrast between the cortex and medulla has been used to infer its intratubular location [48] and to calculate renal concentration ability [38].

Due to the lower rates of tubular fluid flow [49] compared with blood flow, its depiction with CT demands a lower sampling rate (a few seconds of interval between scans) than that necessary for calculation of perfusion. However, using slower scanners would then impede the measurement of concurrent cortical and medullary perfusion.

Hence, the technical capabilities (mainly spatial and temporal resolution) of the various generations of CT scanners, as outlined later here, largely determined the type of studies that could be performed and the accuracy of the renal hemodynamic and functional information obtained.

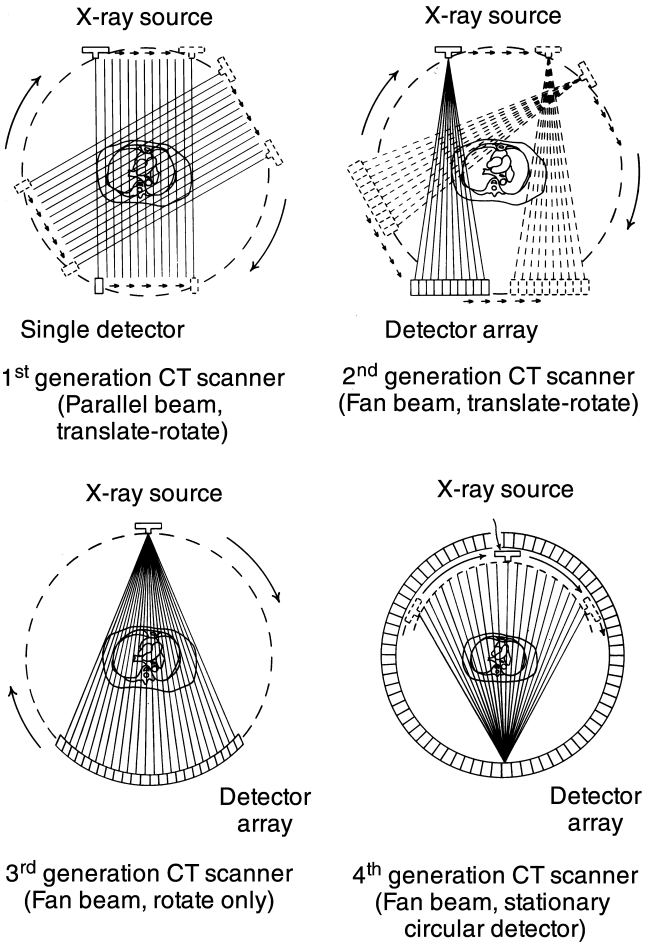

Fig. 5. Diagram demonstrating the evolution of four generations of CT scanners. (From Robb RA: X-ray CT: An engineering synthesis of multiscientific principles. *CRC Crit Rev Biomed Eng* 7:265–334, 1982; used with permission.)

Conventional computed tomography

Conventional CT scanners include the first- and second-generation scanners, which, compared with later generations, have relatively long acquisition times and low temporal resolution.

In the first-generation CT scanners (Fig. 5), the x-ray source is limited to a pencil beam that impacts on two side-by-side detectors [3, 22]. Both the source and the detectors have a translation-rotation movement in order to obtain images from different directions (Fig. 5) [3]. The translation-rotation movement, as well as the pencil beam used, account for the long scanning time (4.5 min) and for the long interscan delay [50]. Second-generation scanners used a fan beam and a detector array (30 detectors) instead of a pencil beam and single detectors (Fig. 5) in order to speed up data acquisition (18 seconds) [22]. However, similar to first-generation scanners, these systems use a translation-rotation movement that limits acquisition speed.

These generations of CT scanners have been useful to assess renal anatomy. Most of these studies were purely anatomical in nature, due to the aforementioned technical constraints. Kidney volume was one of the most commonly studied renal attributes and was measured with high accuracy [51–53]. In addition to anatomical characteristics of the pyelocaliceal system [54], pathological states such as renal infection [55–58], status postlithotripsy [59], and blunt trauma outcomes [60] were also frequently studied with these techniques.

These studies established CT as the first radiographic, noninvasive technique capable of displaying the body internal anatomy in a three-dimensional frame [3, 22], with resolution high enough to allow differentiation between soft tissues. However, because of scanning and interscanning time constraints, it was not possible to include the temporal dimension in the analysis. The capability for dynamic studies was one of the advantages of later generations of CT scanners, thereby providing a completely new insight into physiological and pathophysiological processes.

Dynamic computed tomography

The third and fourth generations of CT scanners constitute the Dynamic CT Scanners, which have improved temporal data acquisition, thanks to improvements in both the x-ray tube and detectors' characteristics (Fig. 5). The third-generation CT scanners have a larger array of detectors (300 detectors, usually circular), with a 360° rotation of both the source and detectors the only movement required for image acquisition and reconstruction (Fig. 5), thereby shortening scanning time (approximately two seconds).

Fourth-generation scanners use a stationary data acquisition system and a fixed circular array of 1,200 to 4,800 detectors [61]. Only the x-ray generator and tube rotate at 360°, thus shortening the scanning time even further (Fig. 5). However, although the temporal resolution of conventional CT scanners is not in the subsecond range, their high-radiation exposure contributes to superior spatial resolution (6 to 8 line-pairs per cm) [34].

Early applications of dynamic CT renal scanning were directed to observe relative contrast media enhancement characteristics in different regions of the kidney and to detect changes that occur under certain pathophysiological situations, such as renovascular hypertension [62], ischemic kidney [29], status post-renal artery dilation [63, 64], and renal insufficiency [41]. Later applications were directed to quantitative assessment of renal hemodynamics, mainly renal blood flow [65–67], volume [68–72], and permeability [45, 46]. However, despite the considerably shortened data-acquisition times, the sampling rate was still too low to record changes of contrast concentration within the renal tubules with adequate accuracy.

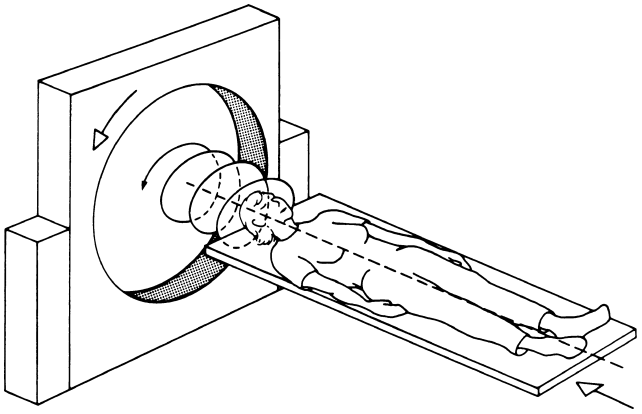

Fig. 6. Scanning geometry in helical (spiral) CT. (From [73] BRINK JA: Technical aspects of helical (spiral) CT. *Radiol Clin North Am* 33:825–841, 1995; used with permission.)

Fast computed tomography

This group of CT scanners includes machines capable of obtaining sequential, subsecond cross-sectional scans and in which the sampling rate is therefore high enough [22] to be used for a more accurate calculation of renal blood flow, as well as indices of tubular function.

Helical computed tomography. In spiral (helical) CT, the x-ray source rotation and patient translation occur simultaneously and continuously (Fig. 6) [73]. This permits scanning of an object in a relatively short period of time, usually during a single breath hold.

Because of the combined rotation-translation movement, images obtained are of nonuniform section thickness and orientation that may complicate the data analysis [74]. To overcome this limitation, interpolation analysis is needed. Usually a 180° interpolation algorithm is used, which results in increased longitudinal resolution [34]. Longitudinal resolution, which is inversely proportional to couch speed and reconstruction intervals, can also be improved using a prolonged scanning time.

Because of the continuous data acquisition and the ability to generate multiple overlapping images, this methodology affords a high-quality, three-dimensional data acquisition and display [34]. However, because of relatively long effective exposure times (approximately one second), its temporal resolution is lower than some other fast CT scanners, and therefore, it is less frequently used for acquisition and analysis of dynamic data.

Several studies have demonstrated the capability of spiral CT to study renal anatomy and function [75, 76]. Parameters studied included kidney volume, renal artery angiography (for renal artery stenosis assessment) [77], surgical planning and focal lesions localization and stadification.

Dynamic spatial reconstructor. As mentioned earlier, the major advantage of the application of CT was that it allowed the tomographic imaging of any cross-section of the human body, such as the chest, abdomen, and legs, thereby enabling characterization of their internal structure. Although this characteristic represents an indisputable and significant advance in disclosing anatomical detail, it does not provide any dynamic information that could disclose organ function. This latter concept has been applied to those organs in which functionality can be assessed by determining the changes in shape or volume such as cardiac contraction [78] or pulmonary ventilation [79] or to those organs whose function is related to the flow of blood or other locally formed fluids. The kidney constitutes a good example of this latter case because changes in blood flow influence the formation of renal tubular fluid volume by altering glomerular filtration rate and/or tubular sodium reabsorption. Measurements of these dynamic parameters necessitate very fast sequential scanning of the same cross-section in such a manner that tissue blood perfusion or tubular fluid flow could be determined by external detection of the transit of a bolus of x-ray-filterable contrast media. In all these cases, the accuracy with which the change in tissue density consequent to transit of contrast can be recorded is closely dependent on the number of images that can be obtained per unit of time (temporal resolution).

The first three-dimensional volume-scanning CT scanner (multiple contiguous slices of a given organ scanned simultaneously) with high temporal resolution (scan repetition rate of up to 60 times/second for up to 20 seconds) was presented in 1980 [80]. This instrument, conventionally called the dynamic spatial reconstructor (DSR), consists of 14 x-ray tubes and 14 television cameras. X-ray tubes are arranged in a semicircular array (each 12° apart), and each tube has a corresponding television camera (opposite to the tube; Fig. 7) that records the scan data.

Initial studies on renal circulation with the DSR demanded a comparison with another technique capable of measuring renal blood flow and its intrarenal distribution. A comparative examination of all methods available at that time to estimate intrarenal distribution of blood flow (such as kripton and xenon washout, kripton autoradiography, H2 electrodes, heat clearances, transit renography, computerized angiography, and radiolabeled microspheres) was published in 1982 [81]. From all these methods, the use of radiolabeled microspheres was considered the "gold standard," as their accuracy to estimate organ flow was well demonstrated [82]. However, there were some serious concerns about the use of microspheres to estimate distribution of blood flow in different areas of the renal cortex. Using a rigid hydrodynamic model, Morkrid et al showed that circulating cells or equivalent elements such as microspheres with high specific gravity tend to occupy the center of the blood

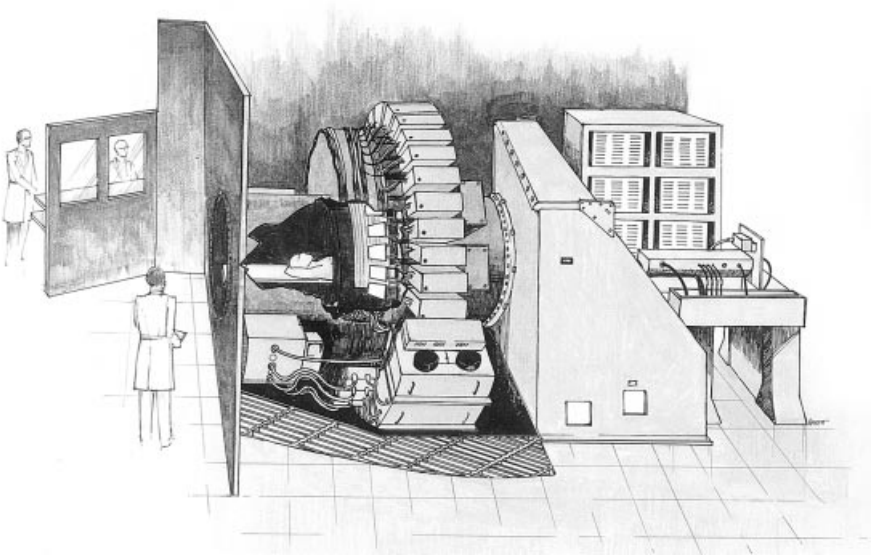

Fig. 7. Artist's representation of the Dynamic Spatial Reconstructor (DSR). (From Bentley MD, Fiksen-Olsen MJ, Knox FG, Ritman EL, Romero JC: The Use of the Dynamic Spatial Reconstructor to study renal function, in *Primary Hypertension*, edited by Kaufmann W, Berlin/Heidelberg, Springer Verlag, 1986, pp 126–141, © 1986 Springer-Verlag; used with permission.)

stream in interlobular arteries, impeding their access to glomerular afferent arterioles in the deep cortex, that depart at right (and even acute) angles from the interlobular artery [83]. Such a phenomenon, called "stereic hindrance" or "plasma skimming," was confirmed with the DSR. In this study, it was shown that microspheres distribute predominantly in the superficial cortex (Fig. 8). However, during renal vasodilation induced by a continuous infusion of bradykinin, microspheres were more uniformly distributed with an increased concentration in the deep cortex and showed better agreement with DSR measurements. These results were interpreted to be the consequence of a fall in circulatory velocity during vasodilation. This leads to cell margination, which facilitates the access of cells or microspheres into juxtamedullary afferent arterioles [84]. These changes mimicked a redistribution of blood flow from the superficial to the deep cortex when actually there was only redistribution of microspheres.

In a study designed to examine the canine renovascular anatomy using the DSR, arterioles as small as 1 mm in diameter were found to be detectable. The machine can also provide detailed dilution curves of the transit of contrast in the four zones of the renal cortex (superficial, middle, inner, and juxtamedullary) and in two different areas (outer and inner) of the renal medulla. From these dilution curves Bentley et al developed a mathematical equation that allowed a precise calculation of renal blood flow [43]. These measurements yielded a correlation of 0.91 when compared with simultaneous measurements made with an electromagnetic flowmeter over a wide range of changes of renal blood flow, such as 10%, 30%, and 50% below the range of renal blood flow autoregulation [43].

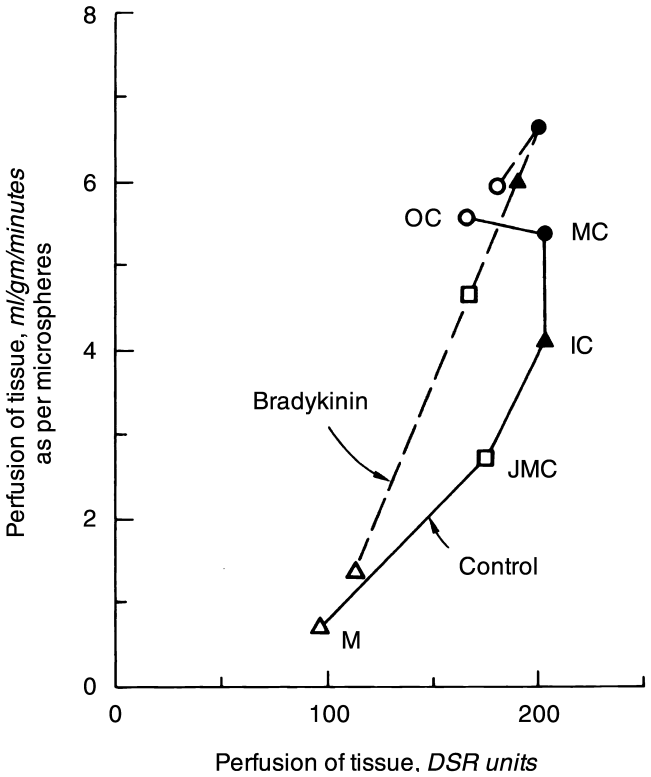

Fig. 8. Regional renal perfusion measured with the dynamic spatial reconstructor (DSR) and with 15 μ radiolabeled microspheres under control conditions and during renal vasodilation, achieved by an intrarenal infusion of bradykinin (0.75 μg/kg/min). Perfusion was measured in the renal medulla (M), juxta-medullary cortex (JMC), and inner (IC), middle (MC), and outer (OC) cortex. In the vasodilated kidney, the microspheres-to-DSR relationship becomes more linear because of the vasodilation-induced decrease in stereic hindrance, leading to more uniform of the microspheres. (From [84] Iwasaki T, Ritman EL, Fiksen-Olsen MJ, Romero JC, Knox JG: Renal cortical perfusion: Preliminary experience with the dynamic spatial reconstructor (DSR). *Ann Biomed Eng* 13:259–271, 1985; used with permission.)

Studies were also performed with the DSR to determine changes in intrarenal distribution of blood flow when renal perfusion pressure was altered within the range of renal blood flow autoregulation (114 to 153 mm Hg). Diversion of blood from superficial (short, salt-losing nephrons) to juxtamedullary (long, salt-saving nephrons) glomeruli had been suggested by Barger to explain the fall of urinary sodium excretion in the absence of changes in total blood flow (within the range of autoregulation) [85]. The results obtained with the DSR demonstrated that changes in renal perfusion pressure were not accompanied by any significant alteration in the distribution of blood flow within the renal cortex [86]. However, under these conditions, a very significant change (34.7%) in the papillary flow was observed, which contrasted with a lack of changes in outer renal medulla [86]. The importance of changes in papillary flow on the regulation of urine sodium excretion was first suggested by Roman and Cowley, who showed with the use of a laser doppler probe that the vasculature of the renal papilla did not exhibit any autoregulation of blood flow [87]. This mechanism allowed the kidney to sense changes in aortic pressure in a small area of the renal parenchyma (medullary flow comprises 4% to 6% of total renal blood flow) without altering the autoregulatory response in the renal cortex and outer medulla. The importance of papillary flow in the regulation of sodium excretion is discussed further in the next section.

In spite of the great potential of the DSR, it was not extensively used, first because the instrument was not available to investigators outside the Mayo Clinic, and second, because of high operating and maintenance costs. However, further studies on intrarenal hemodynamics were made possible when Imatron, a California company, marketed the first commercially available electron beam CT. This instrument is described in the next section.

ELECTRON BEAM COMPUTERIZED TOMOGRAPHY (EBCT)

This instrument represents a novel concept in the use of x-ray to obtain fast three-dimensional tomographic scanning. The major differences between the EBCT and the DSR or conventional CT is that EBCT has no mechanical parts (x-ray tubes and/or TV cameras) moving around the patients, resulting in lower heat production and enabling fast scanning. An electron beam, originating from an electron gun located behind the patient (Fig. 9), is magnetically deflected sequentially onto four tungsten target rings, producing eight fan beams (2 from each target ring) of x-ray radiation that pass through the patient (Fig. 9). The kidney can then be imaged by eight almost simultaneous cuts that are thicker than those produced by the DSR (8 mm). Alternatively, consecutive 1.5, 3, or 6 mm thick tomographic slices can be obtained by using a single target ring and moving the patient table at predetermined increments. Although its temporal resolution is lower than the DSR (50 or 100 msec/image), this resolution is nonetheless sufficient to obtain adequate evaluation of renal function. Furthermore, because of the slightly longer scan duration and lower image noise compared with the DSR, its spatial resolution is better, although lower than conventional CT (2 to 4 line pairs/cm) [34].

Jaschke et al were the first to demonstrate the potential of the EBCT in measuring renal blood flow and to establish the basic principles for that calculation that correlated highly with measurements obtained with radioactive microspheres [35, 88]. Subsequent validation studies demonstrated the accuracy of EBCT-derived measurements of renal, cortical, and medullary (compared with their *in vitro*) volumes [32], perfusion (compared with electromagnetic flowmetry) within a wide range of renal blood flow values [89], as well as changes in blood flow distribution [38].

DETERMINATION OF TUBULAR DYNAMICS

An important step in evaluating renal function was the description of the dynamic characteristics of tubular fluid transit through different nephron segments, using inulin-like contrast medium as a marker [38]. The scanning sequence was designed so as to first follow the transit of x-ray contrast through renal vasculature in the cortex and in the medulla. After completion of the first pass of the bolus through the kidney (5 to 6 sec), a residual opacity is observed (Fig. 10), that, as interpreted by Jaschke [29], corresponds mainly to contrast that has been filtered in the glomeruli and is contained in the proximal tubules. Continuing the scanning sequence at few second intervals, the displacement of this contrast medium through the nephron can be traced. Potts et al were the first to measure the transit times between two different regions of the canine kidney from EBCT contrast attenuation curves [48]. From their recent report and ours [38], it can be concluded that these displacements indicate the flow of contrast medium along the different nephron segments (Fig. 10), that is to say, from the proximal tubules (cortex) to the descending (outer medulla) portion of the loop of Henle, the tip (inner medulla) and the ascending portion of the loop of Henle (outer medulla), returning to the distal tubule cortex, after which it is cleared through the collecting system, located in cortex, medulla, and renal pelvis (Fig. 10). Furthermore, the transit time of contrast media displacement through all of these renal segments agreed closely with those measured in dogs by Steinhouser et al using lisamine green [90, 91]. The contrast also showed changes in density similar to those described for inulin, whose

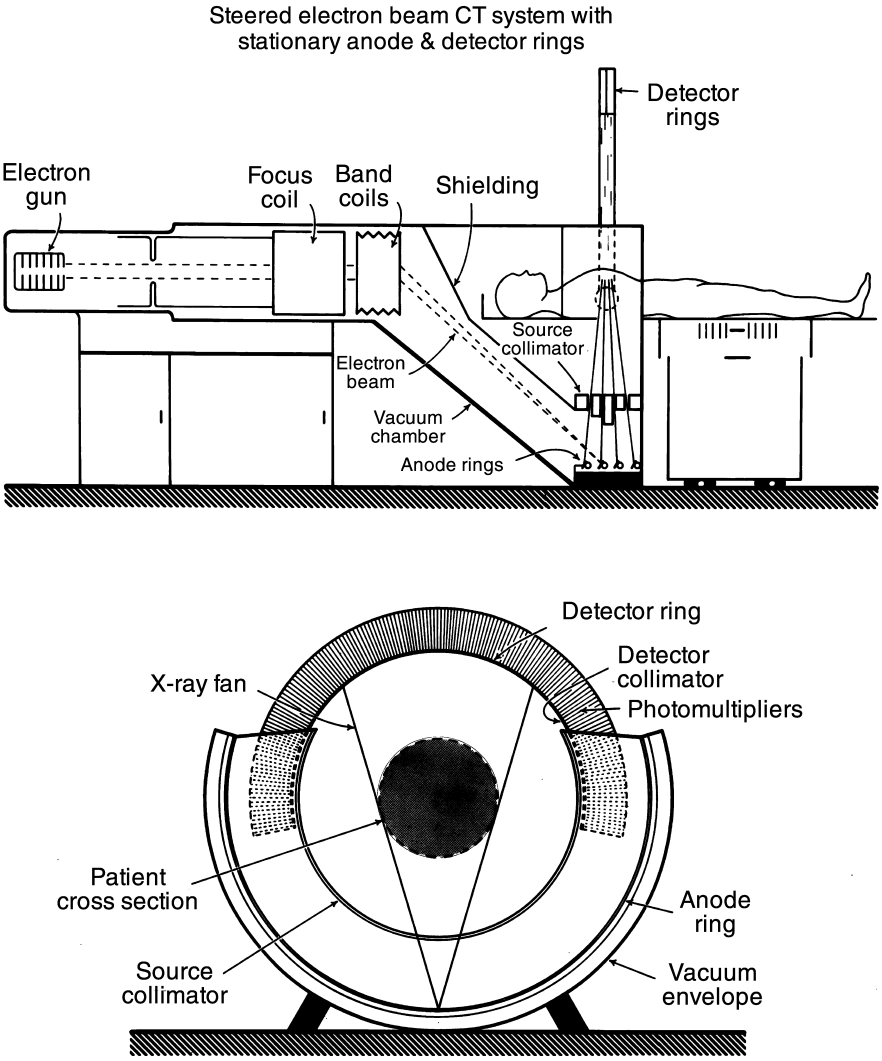

Fig. 9. Diagram of cardiovascular computed tomographic (CVTC) system. (*Top*) Longitudinal section of system showing deflection and focusing of electron beam onto fixed semicircular anode ring, and collimator assembly to generate data for eight adjacent sections as beam is rapidly sequenced from point-to-point along each of four anode rings. (*Bottom*) End view of system showing relationship of patient cross section to fixed detector arc and electronically swept x-ray fan beam source (From Boyd DP, Gould RG, Quinn JK, Sparks R, Stanley JH, Herrmannsfeldt WB: *IEEE Trans Nucl Sci* NS-26(2), 2724, 1979, © 1979 IEEE, and modified by Robb RA: *CRC Crit Rev Biomed Eng* 7:319, 1982; used with permission.)

concentration progressively increases toward the tip of the papilla (because of the osmotic gradient) and redilutes as it returns to the cortex through the thick ascending loop of Henle. This suggested that changes in tubular fluid and mostly sodium reabsorption in a given tubular segment can be detected by corresponding changes in the density of contrast medium and by proportional alteration in the transit time. To test this assumption, the kidney was scanned during the administration of furosemide [38], a loop-diuretic that decreases sodium chloride reabsorption in the ascending loop of Henle [92]. Figure 11 demonstrates a corresponding significant contrast dilution (or fall in x-ray density) in the loop of Henle and collecting system that was detected with EBCT.

These resulted in the conclusion that EBCT constitutes an excellent method to determine accurate changes in intrarenal distribution of blood flow and the manner in which these changes are coupled to changes in tubular sodium excretion [38].

This observation encouraged Rodriguez et al to determine the changes in intrarenal distribution of blood flow and tubular dynamics that occur during alterations of renal perfusion pressure within the range of renal autoregulation [93]. The results of these studies were largely confirmatory of a previous observation made with the DSR, in that there were no changes in the cortical distribution of blood flow, whereas papillary flow changed in direct proportion to renal perfusion pressure. However, a careful measurement of all the hemodynamic changes in the inner medulla was performed to examine how extensive an area was involved in these alterations. It was found that there was an area of the inner medulla that lies immediately outward to the papilla that exhibited changes in flow opposite to those seen in the papilla. In other words, the increments in papillary flow were counteracted by opposite directional changes in this outlying papillary zone.

Because of these opposite changes in two closely re-

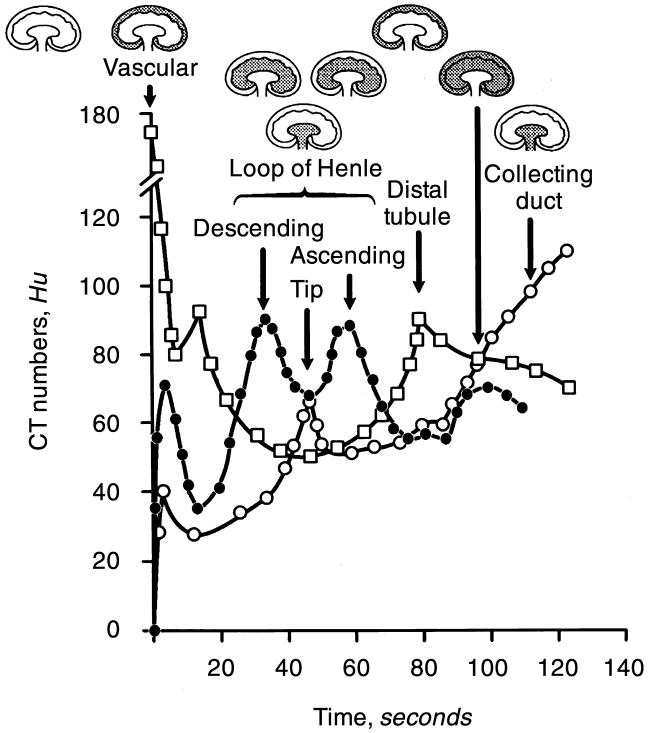

Fig. 10. Time-density curves obtained in a canine kidney during the transit of a bolus of a filterable contrast medium (iopamidol). The curves were obtained separately from the renal cortex (□), outer medulla (●), and inner medulla (○), and each peak represents intratubular contrast sequentially transversing the nephron segments contained in these regions. At the top of the figure, the corresponding anatomic location of the contrast in the renal cross-sectional regions is illustrated.

lated areas, the change in total medullary flow was not statistically significant. Nevertheless, the small changes in papillary flow were positively correlated with the amount of sodium excreted in the urine [38].

The previously mentioned alterations in the inner medulla induced by changes of renal perfusion pressure within the range of renal blood flow autoregulation were accompanied by significant decrements of sodium reabsorption in proximal, late proximal, thick ascending, and cortical distal tubules. The relationship between these rather large changes in tubular fluid reabsorption with relatively small circulatory alterations circumscribed to the inner papilla need to be explored further. It will be interesting to know if, as suggested by Roman et al [87], changes in renal papilla alter the interstitial pressure, thereby inducing modifications in tubular sodium reabsorption through the release of humoral substances (such as nitric oxide and prostaglandins) or, if on the contrary, the hemodynamic changes alter nitric oxide synthesis (mediated by shear stress) and thereby sodium reabsorption, producing intratubular fluid expansion. This tubular fluid expansion will alter interstitial pressure, which can modify medullary circulation through changes in capillary wall tension. In this latter case, the changes in papillary flow will be the consequence, not the cause, of the changes in tubular fluid resorption.

INTRARENAL HEMODYNAMICS IN THE NORMAL AND HYPERTENSIVE HUMAN'S KIDNEY

Using methodology developed in animal studies [32, 38, 89], EBCT estimates of the whole kidney, cortical, and medullary perfusions and volumes have been shown to be feasible and highly reproducible in normal humans under controlled conditions [94]. Similar principles were applied in recent years in a series of EBCT studies aimed to investigate intrarenal perfusion and volume in essential and renovascular hypertension. Normotensive humans with a family history of essential hypertension [95], as well as essential hypertensive patients [96], were found to have normal regional renal volumes but a significantly lower cortical perfusion compared with humans without such a predisposition. In patients with renovascular hypertension and preserved renal function, cortical and medullary perfusion correlated inversely with the degree of stenosis in fibromuscular dysplasia, but not in atherosclerotic renal artery stenosis. In fact, the decrease in cortical perfusion in the latter exceeded in severity the degree of the stenosis, underscoring the systemic nature of atherosclerosis [96]. Future studies of renal tubular dynamics in animal and human models of hypertension may potentially shed light on the nephron sites and the degree of impairment of renal function in this disease.

LIMITATION OF CT SCANNING AND OTHER X-RAY TECHNIQUES

Limitations of CT can be divided into data acquisition related (imaging artifacts, contrast media) and patient safety related (radiation exposure and contrast media).

Imaging artifacts

X-ray imaging may be associated with artifacts such as "partial volume effect" (*vida supra*), "beam hardening" (an artificial increase in the average energy of the transmitted beam), and photon scatter (caused by detection of x-ray information originating outside the x-ray source and detector plane) [33]. These can be partly corrected or avoided by adopting simple precautions, and are being addressed in the newer generations of CT scanners (fast CT).

Radiation exposure

The entrance radiation exposure incurred with conventional CT is 1.9 rads/second, compared with 10 rads/second for EBCT [3]. However, because of the short scanning time of EBCT, this dosimetry translates into about 1 rad for each high-resolution scan (100 msec/

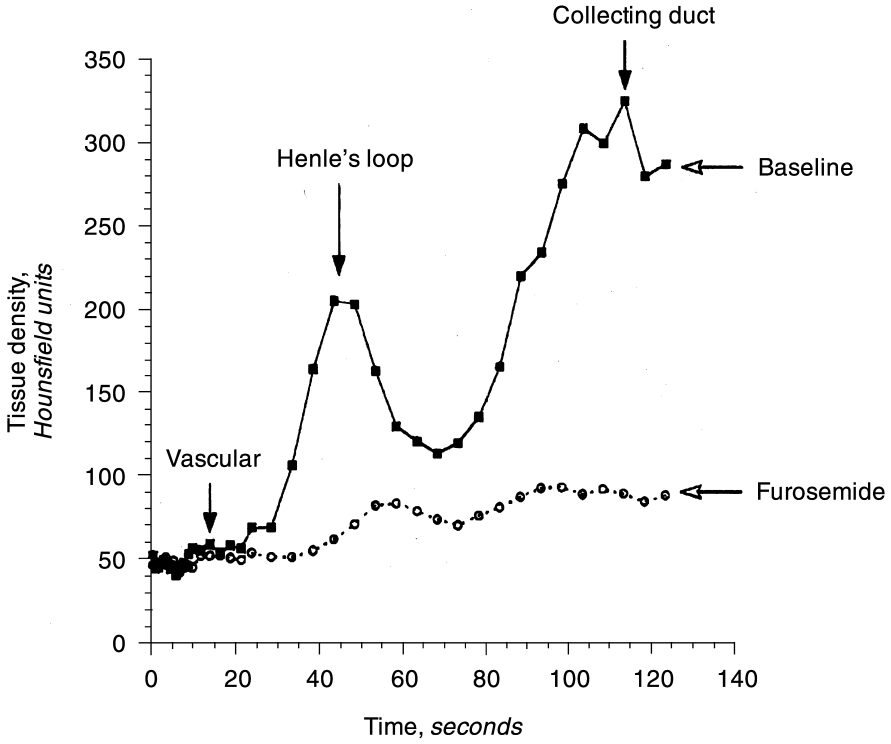

Fig. 11. Time density curves obtained with electron beam computerized tomography (EBCT) in the renal inner medulla before (solid squares) and after (circles) systemic administration of furosemide. This loop-diuretic induced a marked dilution (and hence a decrease in tissue densities) in the nephron segments from the loop of Henle and distally, which was detectable with EBCT.

image) and approximately 0.5 rad for a standard resolution scan (50 msec/image).

Contrast media

Most of the contrast media routinely used for x-ray examinations are derivatives of a benzene ring, which absorbs x-rays thanks to the presence of iodine atoms [36].

Radiographic contrast agents are removed from circulation primarily via glomerular filtration and are not secreted or reabsorbed in the kidney [36]. In that regard, contrast media behave like inulin, with the advantage that they can be externally detected. Due to their high osmolarity, their presence in the kidney may lead to diuresis, tubular expansion, and an increase in renal size [97]. Their high osmolarity also renders them potent systemic vasodilators, and their use is often accompanied by a transient fall in blood pressure [98]. As opposed to the systemic vasculature, the response of the kidney to conventional contrast media is characteristically biphasic. A transient vasodilation, similar to contrast-induced blood flow changes in other vascular beds, is followed by a more prolonged vasoconstriction unique for the renal vascular bed [99]. Contrast media may also decrease the glomerular ultrafiltration coefficient (Kf) and glomerular filtration rate, a tubuloglomerular feedback phenomenon initiated by delivery of high-solute tubular contents to the macula densa [99]. However, because most of these adverse effects are due to the high osmolarity of conventional contrast media, these are minimized with the use of low-osmolar contrast agents [100, 101], which have little effect on renal perfusion and function and are therefore preferable agents for physiological studies. In addition, the fact that CT-derived renal perfusion and function remain unaltered in time-control animals and are highly correlated with independent measures obtained by "gold standards" affirms their reliability as indicators.

CONCLUSION

In conclusion, x-ray techniques in general and CT scanners in particular offer a unique insight into the synchronous intrarenal hemodynamics and function, allowing noninvasive investigation of their interdependence. This may provide an almost unprecedented opportunity to elucidate mechanisms associated with shifts in the pressure-natriuresis curve, development of hypertension, renal disease mechanisms, and more. Future development of automated data analysis software may enable taking advantage of this technology for routine clinical purposes.

ACKNOWLEDGMENTS

This work was supported by National Institutes of Health grants HL16496 and HL03621 and by the Mayo Foundation. The authors are grateful to Kristy Zodrow for preparation of this manuscript.

Reprint requests to Juan Carlos Romero, M.D., Mayo Clinic, Department of Physiology, 200 First Street SW, Rochester, Minnesota 55905, USA.

REFERENCES

1. Roentgen WC: Ueber eine neue art von Strahlen. *Annalen der Physic und chemie* 1–37, 1898
2. Carelli HH, Sordelli E: A new procedure for examining the kidney. *Rev Assoc Med Argent* 34:18–19, 1921
3. Robb RA, Morin RL: Principles and instrumentation for dynamic x-ray computed tomography, in *Cardiac Imaging: A Companion to Braunwald's Heart Disease*, edited by Marcus ML, Schelbert HR, Skorton DJ, Wolf GL, Philadelphia, W.B. Saunders, 1991, pp 634–668
4. Eisenberg RL: Roentgen and the discovery of x-rays, in *Radiology: An Illustrated History*, edited by May CR, St. Louis, Mosby-Year Book, 1992, pp 22–34
5. Eisenberg RL: UroRadiology, in *Radiology: An Illustrated History*, edited by May CR, St. Louis, Mosby-Year Book, 1992, pp 304–322
6. MacIntyre J: Roentgen says: Photography of renal calculus. Description of an adjustable modification in the focus tube. *Lancet* 2:118, 1896
7. Tuffier T: Sonde ureterale opaque, in *Duplay et Reclus: Traite de Chirurgie*, Paris, Masson 1897–1899, pp 412–413
8. Von Illes G: Ureteral catheterization and roentgenography. *Orv Hetil* 45:659–662, 1901
9. Braasch WF: Pyelography: A study of the normal and pathologic anatomy of the renal pelvis and ureter, in *Pyelography*, edited by Braasch WF, Philadelphia, WB Saunders, 1915
10. Osborne EA, Sutherland CG, Scholl J, A J, Rowntree LG: Roentgenography of urinary tract during excretion of sodium iodide. *JAMA* 80:368–373, 1923
11. Wesson MB, Fuller CC: Influence of ureteral stones on intravenous pyelograms. *Am J Radiol* 28:27–33, 1932
12. Evans JA: Nephrotomography in the investigation of renal masses. *Radiology* 69:684–689, 1957
13. Trueta J, Barclay AE, Daniel PM, Franklin KJ, Prichard MML: *Studies of the Renal Circulation*, Springfield, Thomas C.C., 1947, pp 1–181
14. Erikson U, Rhun G, Wolfgast M: Measurement of total and regional blood flow by means of a videodensitometric method. *Scand J Nephrol* 29(Suppl):101–103, 1975
15. Erikson U, Lidgren PG, Lofroth PO, Ruhn G, Wolfgast M: Measurement of total and regional renal blood flow measurement. *Acta Radiol Diagnosis* 18:225–234, 1973
16. Erikson U, Lörelius LE, Ruhn G, Wolfgast M: Regional renal function measured by videodensitometry. *Scand J Urol Nephrol* 15:131–135, 1981
17. Ovitt TW, Christenson PC, Fisher I, H D, Frist MM, Nudelman S, Roehrig H, Seeley G: Intravenous angiography using digital video subtraction: X-ray imaging system. *Am J Radiol* 135:1141–1144, 1980
18. Hillman B: Digital radiologic monitoring of renal physiology. *The Physiologist* 26:35–38, 1983
19. Eisenberg RL: Tomography, in *Radiology: An Illustrated History*, edited by May CR, St. Louis, Mosby Year Book, 1992, pp 430–436
20. Vallebona A: A modified technique roentgenographic dissociation of shadows applied to the study of the skull. *Radiol Med* 17:1090–1097, 1930
21. Grossmann G: Lung tomography. *Br J Radiol* 96:733–751, 1935
22. Hounsfield GN: Computed medical imaging. *J Comput Assist Tomogr* 4:665–674, 1980
23. Radon J: Über die Bie Bestimmung von Funktionen durch ihre Integralwerte längs gewisser Mannigfaltigkeiten. *Ber Sachs Akad Wiss Math Phys K1* 69:262–277, 1917
24. Oldendorf WH: Isolated flying spot detection of radiodensity discontinuities: Displaying the internal structural pattern of a complex object. *IRE Trans Biomed Electron* 8:68–72, 1961
25. Cormack AM: Representation of a function by its time integrals, with some radiological applications. *J Appl Phys* 35:2908–2913, 1964
26. Hounsfield GN: Computerized transverse axial scanning (tomography). Part 1. Description of system. *Br J Radiol* 46:1016–1022, 1973
27. Hansell P: Evaluation of methods for estimating renal medullary blood flow. *Renal Physiol Biochem* 15:217–230, 1992
28. Axel L: Cerebral blood flow determination by rapid-sequence computed tomography. *Radiology* 137:679–686, 1980
29. Jaschke W, Lipton MJ, Boyd DP, Cann C, Strauss L, Sievers R: Attenuation changes of the normal and ischemic canine kidney: Dynamic CT scanning after intravenous contrast medium bolus. *Acta Radiol* 26:321–330, 1985
30. Nitzsche EU, Choi Y, Killion D, CK H, Hawkins RA, Rosenthal JT, Buxton DB, Huang SC, Phelps ME, Schelbert HR: Quantification and parametric imaging of renal cortical blood flow in vivo based on Patlak graphical analysis. *Kidney Int* 44:985–996, 1993
31. Bentley MD, Karwoski RA: Estimation of tissue volume from serial tomographic sections: A statistical random marking method. *Invest Radiol* 23:742–747, 1988
32. Lerman LO, Bentley MD, Bell MR, Rumberger JA, Romero JC: Quantitation of the in vivo kidney volume with cine computed tomography. *Invest Radiol* 25:1206–1211, 1990
33. Rumberger JA, Bell MR, Feiring AJ, Behrenbeck T, Marcus ML, Ritman EL: Measurement of myocardial perfusion using fast computed tomography, in *Cardiac Imaging: A Companion to Braunwald's Heart Disease*, edited by Marcus M, Schelbert H, Skorton D, Wolf G, Philadelphia, W.B. Saunders, 1991, pp 688–702
34. McCollough CH, Robb RA: Ultrafast computed tomography: Principles and instrumentation, in *Marcus Cardiac Imaging*, edited by Skorton DJ, Schelbert HR, Philadelphia, W.B. Saunders, 1996, pp 793–819
35. Jaschke W, Gould R, Assimakopoulos PA, Lipton MJ: Flow measurements with a high-speed computed tomography scanner. *Med Phys* 14:238–243, 1987
36. Morris TW, Fischer HW: The pharmacology of intravascular radiocontrast media. *Ann Rev Pharmacol Toxicol* 26:143–160, 1986
37. Blomley MJ, Dawson P: Review article: The quantification of renal function with enhanced computed tomography. *Br J Radiol* 69:989–995, 1996
38. Lerman LO, Rodriguez-Porcel M, Sheedy PFI, Romero JC: Renal tubular dynamics in the intact canine kidney. *Kidney Int* 50:1358–1362, 1996
39. Dawson P, Peters AM: Functional imaging in computed tomography: The use of contrast-enhanced computed tomography for the study of renal function and physiology. *Invest Radiol* 28:S79–S84, 1993
40. Ishikawa I, Onouchi Z, Saito Y, Kitada H: Renal cortex visualization and analysis of dynamic CT curves of the kidney. *J Comput Assist Tomogr* 5:695–701, 1981
41. Ishikawa I, Masuzaki S, Saito T, Tateishi K, Kitada H, Yuri T, Shinoda A, Onouchi Z, Saito Y, Futyu Y: Dynamic computed tomography in acute renal failure: Analysis of time-density curves. *J Comput Assist Tomogr* 9:1097–1102, 1985
42. Probst P, Link L, Futterlieb A, Wehrli HP: Experimental acute renal artery stenosis: Dynamic CT and renal perfusion. *Invest Radiol* 19:87–95, 1984
43. Bentley MD, Lerman LO, Hoffman EA, Fiksen-Olsen MJ, Ritman EL, Romero JC: Measurement of renal perfusion and blood flow with fast computed tomography. *Circ Res* 74:945–951, 1994
44. Lumsden CJ, Silverman M, Zielinski A, Potts DG, Shafik I, Brody AS, Whiteside CI, Violante M: Vascular exchange in the kidney: Regional characterization by multiple indicator tomography. *Circ Res* 72:1172–1180, 1993
45. Miles KA, Kelley BB: CT measurements of capillary permeability within nodal masses: A potential technique for assessing the activity of lymphoma. *Br J Radiol* 70:74–79, 1997
46. Dawson P, Peters M: Dynamic contrast bolus computed tomography for the assessment of renal function. *Invest Radiol* 28:1039–1042, 1993
47. Patlak CS, Blasberg RG, Fenstermacher JD: Graphical evalua-

tion of blood-to-brain transfer constants from multiple-time uptake data. *J Cereb Blood Flow Metab* 3:1–7, 1983
48. Potts DG, Brody AS, Shafik IM, Lumsden CJ, Zielinski A, Silverman M, Whiteside CI: Demonstration of renal tubular flow by selective angiographic computed tomography. *Can Assoc Radiol J* 44:364–370, 1993
49. Zum Winkel VK, Hallwachs O, Steinhausen M: Kameraszintigraphie und isotopennephrographic an der hundeniere und deren überprüfung durch die intravitalmikroskopie. *ROFO* 108:382–393, 1968
50. Eisenberg RL: Computed tomography, in *Radiology: An Illustrated History*, edited by May CR, St. Louis, Mosby Year Book, 1992, pp 467–471
51. Heymsfield SB, Fulenwider T, Nordlinger B, Barlow R, Sones P, Kunter M: Accurate measurement of liver, kidney and spleen volume and mass by computerized axial tomography. *Ann Intern Med* 90:185–187, 1979
52. Yokoyama M, Watanabe K, Inatsuki S, Ochi K, Takeuchi M: Measurement of renal parenchymal volume using computed tomography. *J Comput Assist Tomogr* 5:975–977, 1982
53. Shultz M: Acute changes in renal size in normal and hypertensive dogs. *J Urol* 104:629–634, 1970
54. Heyns CF, van Gelderen WFC: 3-dimensional imaging of the pyelocaliceal system by computerized tomographic reconstruction. *J Urol* 144:1335–1338, 1990
55. Senn E, Zaunbaer W, Bandhauer K, Haertel M: Computed tomography in acute pyelonephritis. *Br J Urol* 59:118–121, 1987
56. Tsugaya M, Hirao N, Sakagami H, Iwase Y, Watase H, Ohtaguro K, Washida H: Computerized tomography in acute pyelonephritis: The clinical correlations. *J Urol* 144:611–613, 1990
57. Meyrier A, Condamin M-C, Fernet M, Labigne-Rousell A, Simon P, Callard P, Rainfray M, Soilleux M, Groc A: Frequency of development of early cortical scarring in acute primary pyelonephritis. *Kidney Int* 35:696–703, 1989
58. Soulen MC, Fishman EK, Goldman SM: Sequelae of acute renal infections: CT evaluation. *Radiology* 173:423–426, 1989
59. Sacks EM, Fajardo LL, Hillman BJ, Drach GW, Gaines JA, Claypool HR, Clinger NJ, Fillmore DJ, Hunt KR, Pond GD: Prospective comparison of plain abdominal radiography with conventional and digital renal tomography in assessing renal extracorporeal shock wave lithotripsy patients. *J Urol* 144:1341–1346, 1990
60. Lupetin AR, Mainwaring BL, Daffner RH: CT diagnosis of renal artery injury caused by blunt abdominal trauma. *AJR Am J Roentgenol* 153:1065–1068, 1989
61. Barnes GT, Lakshminarayanan AV: Conventional and spiral computed tomography: Physical principles and image quality considerations, in *Computed Body Tomography with MRI Correlation*, edited by Lee KTL, Sagel SS, Stanley RJ, Heiken JP, Philadelphia, Lippincott-Raven, 1996, pp 1–20
62. Heinz ER, Dubois PJ, Drayer BP, Hill R: A preliminary investigation of the role of dynamic computed tomography in renovascular hypertension. *J Comput Assist Tomogr* 4:63–66, 1980
63. Probst P, Mahler F, Roesler H, Fuchs WA: Renal artery stenosis and evaluation of the effect of endoluminal dilatation: Comparison of dynamic CT scanning and I-131-OIHA renogram. *Invest Radiol* 18:264–271, 1983
64. Mukai J, Sabel P: Application of dynamic computed tomography to physiologic imaging of renal artery stenosis before and after angioplasty. *Am J Physiol Imaging* 1:33–43, 1986
65. Young SW, Noon MA, Marincek B: Dynamic computed tomography time-density study of normal human tissue after intravenous contrast administration. *Invest Radiol* 16:36–39, 1981
66. Miles KA: Measurement of tissue perfusion by dynamic computed tomography. *Br J Radiol* 64:409–412, 1991
67. Gur D, Yonas H, Wolfson J, S K, Wozney P, Colsher JG, Good WF, Good BC, Herbert DL, Cook EE: Xenon/CT blood flow mapping of the kidney and liver. *J Comput Assist Tomogr* 8:1124–1127, 1984
68. Brenner DE, Whitley NO, Ouk TL, Aisner J, Wiernik P, Whitley J: Volume determinations in computed tomography. *JAMA* 247:1299–1302, 1982
69. Rigauts H, Marchal G, Baert AL, Hupke R: Initial experience with volume CT scanning. *J Comput Assist Tomogr* 14:675–682, 1990
70. Breiman RS, Beck JW, Korobin M, Glenny R, Akwari OE, Heaston DK, Moore AV, Ram PC: Volume determinations using computed tomography. *AJR Am J Roentgenol* 138:329–333, 1982
71. Staron RB, Ford E: Computed tomographic volumetric calculation reproducibility. *Invest Radiol* 21:272–274, 1986
72. Moss AA, Friedman MA, Brito AC: Determination of liver, kidney and spleen volumes by computed tomography: An experimental study in dogs. *J Comput Assist Tomogr* 5:12–14, 1981
73. Brink JA: Technical aspects of helical (spiral) CT. *Radiol Clin North Am* 33:825–841, 1995
74. Heiken JP, Brink JA, Vannier MW: Spiral (helical) CT. *Radiology* 189:647–656, 1993
75. Rubin GD, Silverman SG: Helical (spiral) CT of the retroperitoneuim. *Radiol Clin North Am* 33:903–932, 1995
76. Platt JF, Ellis JH, Reige KA: Assessment of renal function with computed tomographic densitometry measurements. *Acad Radiol* 3:718–723, 1996
77. Rubin GD, Dake MD, Napel S, Jeffrey J, R B, McDonnel CH, Sommer FG, Wexler L, Williams DM: Spiral CT of renal artery stenosis: Comparison of three-dimensional rendering techniques. *Radiology* 190:181–189, 1994
78. Ritman EL, Harris LD, Kinsey JH, Robb RA: Computed tomographic imaging of the heart: The dynamic spatial reconstructor. *Radiol Clin North Am* 18:547–555, 1980
79. Hoffman EA, Sinak LJ, Robb RA, Ritman EL: Non-invasive quantitative imaging of shape and volume of lungs. *J Appl Physiol* 54:1414–1421, 1983
80. Ritman EL, Kinsey JH, Robb RA, Gilbert BK, Harris LD, Wood EH: Three-dimensional imaging of the heart, lungs, and circulation. *Science* 210:273–280, 1980
81. Knox FG, Ritman EL, Romero JC: Intrarenal distribution of blood flow: Evolution of a new approach to measurement. *Kidney Int* 25:473–479, 1984
82. Katz MA, Blantz RC, Rector FC, Seldin DW: Measurement of intrarenal blood flow. I. Analysis of microsphere method. *Am J Physiol* 220:1903–1913, 1971
83. Morkrid L, Ofstad J, Willassen Y: Effects of steric reconstriction on the intracortical distribution of microspheres in the dog kidney. (abstract) *Circ Res* 39:608, 1976
84. Iwasaki T, Ritman EL, Fiksen-Olsen MJ, Romero JC, Knox FG: Renal cortical perfusion: Preliminary experience with the dynamic spatial reconstructor (DSR). *Ann Biomed Eng* 13:259–271, 1985
85. Barger AC: Renal hemodynamic factors in congestive heart failure. *Ann NY Acad Sci* 139:276–284, 1966
86. Lerman LO, Bentley MD, Fiksen-Olsen MJ, Strick DM, Ritman EL, Romero JC: Pressure dependency of canine intrarenal blood flow within the range of autoregulation. *Am J Physiol* 268(*Renal Fluid Electrol Physiol* 37):F404–F409, 1995
87. Roman RJ, Cowley AW Jr, Garcia-Estañ J, Lombard JH: Pressure-diuresis in volume-expanded rats: Cortical and medullary hemodynamics. *Hypertension* 12:168–172, 1988
88. Jaschke W, Cogan MG, Sievers R, Gould R, Lipton MJ: Measurement of renal blood flow by cine computed tomography. *Kidney Int* 31:1038–1042, 1987
89. Lerman LO, Bell MR, Lahera V, Rumberger JA, Sheedy PF, Sanchez Fueyo A, Romero JC: Quantification of global and regional renal blood flow with electron beam computed tomography. *Am J Hypertens* 7:829–837, 1994
90. Steinhausen M, Tanner GA: Microcirculation and tubular urine flow in mammalian kidney cortex (in vivo microscopy), in *Sitzungsberichte der Heidelberger Akademie der Wissenschafter, Mathematisch-naturwissenschaftliche Klasse*, edited by Abhandlung HL, New York, Jahrgang, 1976, p 3
91. Steinhausen M, Hill E, Parekh N: Intravital microscopical studies of the tubular urine flow in the conscious rat. *Pflügers Arch* 362:261–264, 1976
92. Mertz JI, Burnett JC Jr, Knox FG: Diuretic therapy in congestive heart failure, in *Cardiology: Fundamentals and Practice*, ed-

ited by Brandenburg R, Fuster V, Giuliani W, McGoon D, Chicago, Year Book Publishers, 1987, pp 560–565
93. Rodriguez-Porcel M, Lerman LO, Sheedy PF, Romero JC: Perfusion pressure dependency of in vivo renal tubular dynamics. *Am J Physiol* (in press)
94. Lerman LO, Flickinger AL, Sheedy PF, Turner ST: Reproducibility of human kidney perfusion and volume determinations with electron beam computed tomography. *Invest Radiol* 31:204–210, 1996
95. Flickinger AL, Lerman LO, Sheedy PF, Turner ST: The relationship between renal cortical volume and predisposition to hypertension. *Am J Hypertens* 9:779–786, 1996
96. Lerman LO, Taler SJ, Textor S, Sheedy PF, Stanson AW, Romero JC: CT-derived intra-renal blood flow in renovascular and essential hypertension. *Kidney Int* 49:846–854, 1996
97. Lerman LO, Bentley MD, Bell MR, Rumberger JA, Sheedy PF, Romero JC: The effect of a low-osmolar radiographic contrast medium on in vivo and postmortem renal size. *Invest Radiol* 26:992–997, 1991
98. Grainger RG: Osmolality of intravascular radiological contrast media. *Br J Radiol* 53:739–746, 1980
99. Porter GA: Effects of contrast agents on renal function. *Invest Radiol* 28:S1–S5, 1993
100. Schwab SJ, Hlatky MA, Pieper KS, Davidson CJ, Morris KG, Skelton TN, Bashore TM: Contrast nephrotoxicity: A randomized controlled trial of a non-ionic and a ionic radiographic contrast agent. *N Engl J Med* 320:149–153, 1989
101. Gerber KH, Higgins CB: Comparative effects of ionic and nonionic contrast materials on coronary and peripheral blood flow. *Invest Radiol* 17:292–298, 1982